Optical Properties of the Carbon-Modified TiO_2 Prepared by Microwave Carbonization Process

Taro Sonobe, Jaturong Jitputti[1], Kan Hachiya[3],

Tomohiko Mitani, Naoki Shinohara, and Susumu Yoshikawa[1]

Research Institute for Sustainable Humanosphere (RISH), Kyoto University,

Gokasho, Uji, Kyoto 611-0011, Japan

[1] Institute of Advanced Energy (IAE), Kyoto University,

Gokasho, Uji, Kyoto 611-0011, Japan

[3] Graduate School of Energy Science, Kyoto University,

Gokasho, Uji, Kyoto 611-0011, Japan

E-mail address: sonobe@rish.kyoto-u.ac.jp

Abstract

The carbon-modified TiO_2 were synthesized through microwave carbonization of ethanol by using a domestic microwave oven. This process enabled to form the carbonaceous compounds on the surface of TiO_2 and created several new mid-gap bands into the original bandgap within few minutes operation. The sample showed a remarkable visible-light absorption even at the wavelength of around 800nm. The promotion of photocatalytic activity under visible and ultraviolet (UV) light irradiation were also confirmed by the I_3^- formation in KI aqueous solution. The I_3^- formation rate of carbon-modified TiO_2 per unit mass under visible light is almost 25 times higher than that of pure TiO_2. The mid-gap optical absorption mechanisms were investigated through analysis of absorption edges. It is revealed that surface state change against microwave-treatment time results in different mid-gap optical absorption processes.

KEYWORDS: optical properties, mid-gap band visible light active TiO_2, carbon modified, photocatalyst, microwave

1. Introduction

Photocatalyst of titanium dioxide (TiO_2) has been widely applied for environment purification and defogging due to its cheapness, non-toxicity, and high efficiency [1-7]. It is also one of the most promising photoanode materials for electrolyzing water to produce hydrogen fuel [3-7]. However, due to the wide bandgap of 3.2 eV, its photocatalytic activity is available only under ultraviolet (UV) light at the wavelength of shorter than 400 nm which is a small fraction (about 3-4 %) of total solar spectra on the earth. Therefore, it is necessary to develop the visible-light-active titanium dioxide in order to expand the benefit of sunlight for photocatalytic activity and give rise to its wider practical application for environmental purification as well as hydrogen production. Recently, it was discovered that elemental substitution of oxygen with nitrogen in TiO_2 enabled to achieve the photcatalytic activity under visible light irradiation [8-9]. At present, the reason for visible light photcatalytic activity is usually considered to be due to the decrease of bandgap, which is attributed to either mixing the nitrogen 2p states with O 2p states or creation of a N-induced mid-gap bands [8-10]. Whereas, it is considered that the narrowing bandgap as well as creation of new mid-gap bands into original bandgap by chemical doping are one of the main principles to develop the visible-light-active photocatalyst.

Recently, several strategies to produce the visible-light-active TiO_2 by doping with transition metal [11-12] and nonmetal dopants such as C [13-19], N [8-10, 20-21] and S [22] have been proposed. Among them, carbon doping was reported to be effective to improve the photocatalytic activity [16]. To date, various synthesis methods have been studied for obtaining the carbon doped TiO_2, such as sol-gel methods [13-14], thermal oxidation of Ti metal in a natural gas flame [6-7] and the controlled oxidizing TiC powder [15]. Janus *et al*. synthesized the carbon-modified TiO_2 by exposure of TiO_2 to the vapor of ethanol for 1 hour at temperature between 150 and 400 ^oC [16]. Kang *et al*. proposed the mechanochemical and heating operation with ethanol to produce the carbon-modified TiO_2 [17]. Based on their studies, well-controlled heat treatment of TiO_2 powder

with organic solvent enables to create new bonding of Ti-C and C-O on the surface area, which results in visible-light photocatalytic activity. While in the study of bandgap, Shaban *et al*. reported that carbon-modified n-type TiO_2 enhanced excitation possibility for a single photon due to presence of mid-gap band, which contributes to a high photoconversion efficiency under white light [6-7]. From this fact it seems likely that an introduction of mid-gap band into original bandgap of TiO_2 through carbon modification is effective to upgrade its photocatalytic activity under visible light irradiation. However, to the author's best knowledge, there are few detailed studies on the relation between the optical transition mechanisms via mid-gap band and photocatalystic activity of such compounds. This photoexcitation via mid-gap band is expected to be a significant role for the photocatalyitic activity as long as visible light becomes main source of photon energy.

In this study, we synthesized the carbon-modified TiO_2 through microwave carbonization of ethanol by using a domestic microwave oven. This process was very simple, efficient and rapidly produces the carbon-modified TiO_2 with several mid-gap bands. Optical properties of samples were studied to evaluate the role of mid-gap band for its photocatalytic activity under visible light as well as UV light irradiation.

2. Experiments

2.1. Materials

Commercially available TiO_2 powder, Ishihara ST-01, and ethanol were used as starting materials. The TiO_2 powder of 100 mg and 0.25 ml of ethanol were mixed to form the paste precursor, and it was placed on the alumina board with a graphite-powder-embedded insulator (shown in Fig. 1). Several materials such as activation carbon, silicon carbide (SiC), and CuO are known to act as a microwave absorber and exhibit extremely high heating rates under microwave irradiation [23-25]. In this set-up, commercial graphite powder (Wako Pure Chemical Industry) was used as microwave absorber to support microwave heating of the precursor. The sample was

placed at center of domestic microwave oven (2.45 GHz, 600W) and heated for 1 (MW1), 2 (MW2), 3 (MW3), and 6 (MW6) min under atmospheric pressure to obtain carbon-modified TiO_2. After microwave heating, all samples were reground for further characterization.

2.2. Characterization

The UV-Visible (UV-Vis) diffuse reflectance spectra were obtained with a powder UV-Vis spectrophotometer (Shimazu, UV-2450). The Kubelka-Munk function [26-27], $F(R)$, was used as the equivalent of absorption coefficient. This function gives a relationship between the absorption coefficient and the diffuse reflectance,

$$F(R) \propto \alpha/S = (1-R)^2/2R\,, \tag{1}$$

where α is the absorption coefficient, S is the scattering coefficient, and R is the diffuse reflectance. Assuming S is constant, which is usually reasonable around the absorption edge, $F(R)$ is simply proportional to the absorption coefficient.

Attenuated Total Reflectance-Fourier Transform Infrared Spectroscopy (ATR-FTIR) spectra were collected by using FT-IR spectrometer (Perkin-Elmer, Spectrum One) ranged from 400 to 4000 cm^{-1} in wavelength. X-ray diffraction (XRD) analyses were performed on a powder diffractometer (Rigaku, RINT-2100).

2.3. Photocatalytic Activity

The photocatalytic activity was evaluated through the formation of I_3^- in KI aqueous solution. The sample powder of 50 mg was dispersed into 30 ml of aqueous solution with a concentration of 0.2 mol/l in a cylindrical Pyrex vessel. The suspension was mixed with a magnetic stirrer and irradiated by a 300 W xenon lamp (Wakom, KXL-300) with the cutting off filter (Corning CS3-73)

below 420 nm, and 15 W UV light (Vilber Lourmat VL-115L, with a maximum emission at about 365 nm) respectively. The concentration of I_3^- was monitored by UV-Vis spectrophotometer. No I_3^- formation was observed when the experiments were conducted either in the dark or in the absence of the TiO_2 samples.

3. Results and Discussion

3.1. Sample characterization

The ATR-FTIR spectra of the samples are presented in Fig. 2. The large peak at around 1630 cm^{-1} is attributed to the intrinsically absorbed water on the surface of TiO_2 [16-17]. The bands in a region of 1050-1100 cm^{-1} appeared after 1 (MW1) and 2 (MW2) min are attributed to ethoxide (1080 cm^{-1}) and ethanol (1050 cm^{-1}) [17]. After 3 min treatment, these bands are disappeared and new absorption bands are created in a region of 1350-1480 cm^{-1}, which are attributed to CO band (1440 cm^{-1}) and $–CH_3$ band (1378 cm^{-1}), respectively [16]. There is also an absorption bands at around 1550-1610 cm^{-1}, which is possibly ascribed to acetate on the surface [17]. Within the irradiation time studied, these newly appeared bands are decreased after 6 min microwave treatment probably due to their thermal decomposition. The XRD patterns of untreated TiO_2 (ST01), and carbon-modified TiO_2 of MW3 and MW6 are shown in Fig. 3. The carbon-modified TiO_2 shows the same XRD pattern and peak width at (101) with untreated TiO_2 (anatase). It is therefore interpreted that an absorbed ethanol on TiO_2 are carbonized during microwave treatment for 3 min and formed some carbonaceous compounds only on the surface of TiO_2 without changing the crystal structure and crystal size of the sample.

Figure 4 shows UV-Vis absorption coefficients obtained from diffuse reflectance spectra with Kubelka-Munk relation for TiO_2 (ST01), and microwave treated TiO_2 of MW1, MW2, MW3, and MW6. As expected from white color of samples of MW1 and MW2, these samples barely show absorption at the wavelength of 400 nm, which is corresponding to the pure TiO_2. On the other

hand, after 3 min treatment (MW3), it shows a remarkable absorption even at the wavelength of around 800 nm, while 6 min (MW6) mildly shows at the wavelength up to 600 nm. Of particular interest is that the behavior of visible-light response of carbon-modified TiO_2 are accompanied by the changes of surface carbon modification: the absorption of surface carbonaceous compounds increased for the first 3 min of microwave treatment, and then decreased for another 3 min, as seen in Fig. 2. Therefore, it is considered that a visible-light response of carbon-modified TiO_2 by microwave heating, which shows the same behavior against microwave-treatment time as the IR absorption bands above, is attributed to the formation of carbonaceous compounds on the surface. Furthermore, the excessive irradiation of microwave results in the degradation of them on the surface which gives rise to the decrease of visible light response.

3.2. *Photocatalytic I_3^- formation*

Photocatalytic activity under visible light irradiation were investigated by the I_3^- formation in KI aqueous solution. The time-dependent formation profiles of I_3^- under visible light irradiation ($\lambda > 420$ nm) in the suspension of samples are shown in Fig. 5. The I_3^- formation rate of pure TiO_2, and carbon-modified TiO_2 (MW3 and MW6) per unit mass are calculated as 9.09×10^{-6} mol/(g·h), 2.25×10^{-4} mol/(g·h), and 1.25×10^{-4} mol/(g·h), respectively. It can be clearly seen that the visible light photocatalytic activity of carbon-modified TiO_2 prepared by microwave heating are drastically higher than that of pure TiO_2, where the I_3^- formation rate of carbon-modified TiO_2 are almost 25 times higher for MW3 and 14 times higher for MW6 than that of pure TiO_2. This high photocatalytic activity under visible light region is attributed to the high visible light response due to the surface modification by carbonaceous compounds after microwave carbonization of ethanol.

Figure 6 shows the photocatalytic activity under UV light irradiation to investigate the upgrading of photcatalytic nature of TiO_2. The time-dependent formation profiles of I_3^- under UV light irradiation (maximum emission at about 365 nm) in the suspension of samples are shown in

this figure. The I_3^- formation rate of pure TiO_2, and carbon-modified TiO_2 (MW3 and MW6) per unit mass are calculated as 4.82×10^{-5} mol/(g·h), 1.24×10^{-4} mol/(g·h), and 1.69×10^{-4} mol/(g·h), respectively. It was found that the photcatalytic activity for TiO_2 was upgraded even under UV light irradiation by microwave carbonization. However, among the microwave carbon-modified TiO_2, the photocatalytic activity of MW6 is higher than that of MW3, which is contrary to the behavior under visible light irradiation. This implies that the mechanism of electron-hole generation by photoexcitation between MW3 and MW6 is different due to their discrepancy of surface structure.

3.3. Bandgap energy

The absorption edge of microwave carbon-modified TiO_2 can be determined by using the following two fundamental equations:

$$(h\nu\alpha)^2 = \mathrm{C}(h\nu - E_g), \tag{2}$$

$$(h\nu\alpha)^{1/2} = \mathrm{C'}(h\nu - E_g), \tag{3}$$

where $h\nu$ is photon energy (h is Planck's constant and ν is the frequency of light), C and C' are constant, and E_g is bandgap energy. Equation (2) is used for direct transition and eq. (3) for indirect transition [28-29]. The plots of $(\alpha h\nu/S)^2$ and $(\alpha h\nu/S)^{1/2}$ versus photon energy are presented in Figs. 7 and 8 for MW3. These plots suggest that the direct absorption edge is located at 2.8 eV with the indirect absorption edge of another absorption lies at about 1.4 eV within the original bandgap of anatase TiO_2 at 3.2 eV as indicated in Figs. 7 and 8. On the other hand, as can be seen in Fig. 9, MW6 shows two absorption edges of indirect transitions at 1.6 and 2.4 eV. It was found that new mid-gap bands were created into original bandgap after the formation of carbonaceous compounds on the surface for the first 3 min of the microwave treatment and they

showed the different absorption edges respectively. The existence of mid-gap bands in carbon-modified TiO_2 have been indicated by other researchers [6-7]. The mid-gap bands enable the multi-electron excitation by a single photon under UV light irradiation as well as direct excitation by visible light. This results in upgrading the photocatalystic activity of TiO_2. The UV-light excitation also injects carriers into mid-gap bands after the bandgap photoexcitation. Furthermore, the excessive irradiation of microwave causes changing the optical transition mechanism due to the degradation of carbonaceous compounds on the surface as suggested in the ATR-FTIR mesurements. Therefore, the slight difference of photocatalytic activity under UV light irradiation was observed for carbon-modified samples. We assume that the photocatalytic activity enhancement for UV irradiation to MW6 compared with visible light is due to the new gap states for MW6, which consist only of indirect absorptions. This means that the straightforward photoexcitation of carriers to the gap states by visible light has limited possibility because of indirect transitions, while carrier injection via bandgap excitation by UV light and carrier-trapping to the gap states becomes more favorable in turn. As for visible-light-active TiO_2, it seems likely that an introduction of the mid-gap bands with direct absorption edge is effective to the enhanced excitation for photocatalytic activity under visible light irradiation.

4. Conclusion

In summary, we synthesized the carbon-modified TiO_2 through microwave carbonization of ethanol by using a domestic microwave oven. This process enabled to form the carbonaceous compounds on the surface of TiO_2 and created several new mid-gap bands into the original bandgap. The carbon-modified TiO_2 showed remarkable visible-light absorption and photocatalytic activity compared with pure TiO_2. The electron excitation to the mid-gap bands has been enhanced by UV as well as visible light irradiation. In addition, the excessive irradiation of microwave can change the optical transition mechanism due to the degradation of carbonaceous compounds on the surface

which results in the discrepancy of photocatalytic activity under UV and visible light irradiation. As for the 3 min irradiated samples of MW3, the direct absorption edge was located at 2.8 eV with the indirect absorption edge of another absorption lay at about 1.4 eV within the original bandgap of anatase TiO_2 at 3.2 eV, while the 6 min irradiated sample of MW6 showed two absorption edges of indirect transitions at 1.6 and 2.4 eV. We assume that the above discrepancy of photocatalytic activity for MW6 is due to the creation of different gap states during microwave irradiation. This means that the straightforward photoexcitation of carriers to the gap states by visible light has limited possibility under indirect transitions, while carrier injection via bandgap excitation by UV light and carrier-trapping to the gap states becomes more favorable in turn. As for visible-light-active TiO_2, it seems likely that an introduction of the mid-gap bands with direct absorption as an absorption edge is effective to the enhanced carrier excitation for photocatalytic activity under visible light irradiation.

Acknowledgement

The authors would like to express their gratitude to Professor T. Yoko and Associate Professor M. Takahashi at Institute for Chemical Research, Kyoto University, for their support of XRD equipment. Gratitude is forwarded to Professor J. Sugiyama and Dr. Thi Thi Nge at Research Institute for Sustainable Humanosphere, Kyoto University, for their support of ATR-FTIR equipment.

References

[1] A. L. Linsebigler, G. Lu, and J. T. Yater, Jr.: Chem. Rev. **95** (1995) 735.

[2] A. Mills and S. Le Hunte: J. Photochem. Photobiol. A **108** (1997) 1.

[3] M. R. Haffmann, S. T. Martin, W. Choi, and D. W. Bahneman: Chem. Rev. **95** (1995) 69.

[4] A. Fujishima and K. Honda: Nature **238** (1972) 37.

[5] T. Sreethawong, Y. Suzuki, and S. Yoshikawa: J. Solid. State Chem. **178** (2005) 329.

[6] Y. A. Shaban and S. U. M. Khan: Int. J. Hydrogen Energy **33** (2008) 1118.

[7] C. Xu, Y. A. Shaban, W. B. Ingler Jr., and S. U. M. Khan: Sol. Energy Mater. Sol. Cells **91** (2007) 938.

[8] R. Asahi, T. Morikawa, T. Ohwaki, K. Aoki, and Y. Taga: Science **293** (2001) 269.

[9] T. Morikawa, R. Asahi, T. Ohwaki, K. Aoki, and Y. Taga: Jpn, J. Appl. Phys. **40** (2001) L561.

[10] Y. Cong, J. Zhang, F. Chen, and M. Anpo: J. Phys. Chem. C **111** (2007) 6976.

[11] L. Zang, C. Lange, I. Abraham, S. Storck, W. F. Maier, and H. Kisch: J. Phys. Chem. B **102** (1998) 10765.

[12] H. Kisch, L. Zang, C. Lange, W. F. Maier, C. Antonnius, and D. Meissner: Angew. Chem., Int. Ed. **37** (1998) 3034.

[13] S. Y. Treschev, P. W. Chou, Y. H. Tseng, J. B. Wang, E. V. Perevedentseva, and C. L. Cheng: Appl. Catal. B **79** (2007) 8.

[14] Q. Xiao, J. Zhang, C. Xiao, Z. Si, and X. Tan: Sol. Energy **82** (2008) 706.

[15] M. Shen, Z. Wu, H. Huang, Y. Du, Z. Zou, and P. Yang: Mater. Lett. **60** (2006) 693.

[16] M. Janus, M. Inagaki, B. Tryba, M. Toyoda, and A. W. Morawski: Appl. Catal. B **63** (2006) 272.

[17] I. C. Kang, Q. Zhang, S. Yin, T. Sato, and F. Saito,: Appl. Catal. B **80** (2007) 81.

[18] D. Chen, Z. Jiang, J. Geng, Q. Wang, and D. Yang: Ind. Eng. Chem. Res. **46** (2007) 2741.

[19] W. Ren, Z. Ai, F. Jia, L. Zhang, X. Fan, and Z. Zou: Appl. Catal. B **69** (2007) 138.

[20] M. Kitano, K. Funatsu, M. Matsuoka, M. Ueshima, and M. Anpo: J. Phys. Chem. B **110** (2006) 25266.

[21] L. Mei, K. Liang, and H. Wang: Catal. Commun. **8** (2007) 1187.

[22] T. Ohno, M. Akiyoshi, T. Umebayashi, K. Asai, T. Mitsui, and M. Matsumura: Appl. Catal. A **265** (2004) 115.

[23] K. W. Gallis and C. C. Landry: Adv. Mater. **13** (2001) 23.

[24] D. Grossin, S. Marinel, and J. G. Noudem: Ceram. Int. **32** (2006) 911.

[25] M. Susaki: Jpn. J. Appl. Phys. **44** (2005) 866.

[26] P. Kubelka and F. Munk: Z. Tech. Phys. (Leipzig) **12** (1931) 593 [in German].

[27] P. Kubelka: J. Opt. Soc. Am. **38** (1948) 448.

[28] P. Yu and M. Cardona: Fundamentals of Semiconductors (Springer, Heidelberg, 1996).

[29] K. Hachiya, T. Goto, and R. Hagiwara: Electrochim. Acta **53** (2007) 46.

Figure Captions

Fig. 1. Schematic of microwave irradiated set up for carbon modification process: (a) ceramic insulator base ($40 \times 40 \times 10$ mm^3), (b) graphite powder, (c) alumina board, and (d) precursor.

Fig. 2. ATR-FTIR spectra of untreated TiO_2 (ST01), and microwave treated TiO_2 for 1 (MW1), 2 (MW2), 3 (MW3), and 6 min (MW6).

Fig. 3. XRD patterns of untreated TiO_2 (ST01), and microwave treated TiO_2 for 3 (MW3) and 6 (MW6) min.

Fig. 4. UV-Vis absorption coefficients obtained from diffuse reflectance spectra with Kubelka-Munk relation for untreated TiO_2 (ST01), and microwave treated TiO_2 for 1 (MW1), 2 (MW2), 3 (MW3), and 6 (MW6) min.

Fig. 5. Formation profiles of I_3^- as a function of visible light ($\lambda > 420$nm) irradiation time in the suspension of untreated TiO_2 (ST01), and microwave treated TiO_2 for 3 min (MW3) and 6 min (MW6).

Fig. 6. Formation profiles of I_3^- as a function of UV irradiation time in the suspension of untreated TiO_2 (ST01), and microwave treated TiO_2 for 3 min (MW3) and 6 min (MW6).

Fig. 7. The plot of $(\alpha h\nu/S)^2$ vs photon energy for the absorption edge of MW3 denoted by the solid curve. The dotted line is visual guides for $\alpha h\nu \propto (h\nu - E')^{1/2}$ and to evaluate the absorption threshold ($E' = E_g$ for bandgap absorption).

Fig. 8. The plot of $(\alpha h\nu/S)^{1/2}$ vs photon energy for the absorption edge of MW3 denoted by the solid curve. The dotted line is visual guides for $\alpha hv \propto (hv\text{-}E')^2$ and to evaluate the absorption threshold ($E' = E_g$ for bandgap absorption).

Fig. 9. The plot of $(\alpha h\nu/S)^{1/2}$ vs photon energy for the absorption edge of MW6 denoted by the solid curve. The dotted line is visual guides for $\alpha hv \propto (hv\text{-}E')^2$ and to evaluate the absorption threshold ($E' = E_g$ for bandgap absorption).

Figures

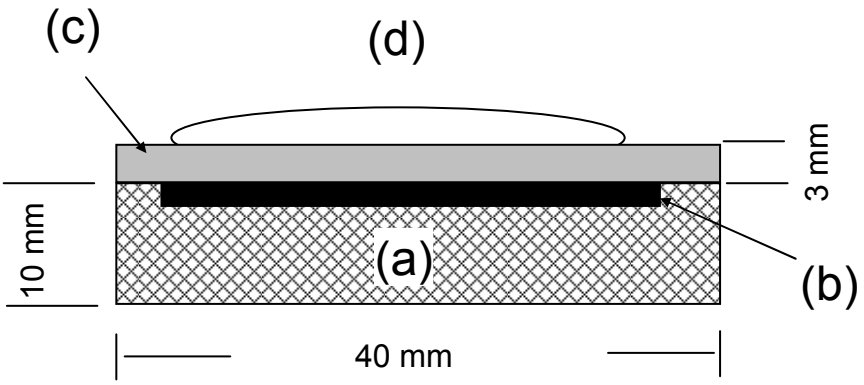

Fig. 1. Schematic of microwave irradiated set up for carbon modification process: (a) ceramic insulator base ($40 \times 40 \times 10$ mm^3), (b) graphite powder, (c) alumina board, and (d) precursor.

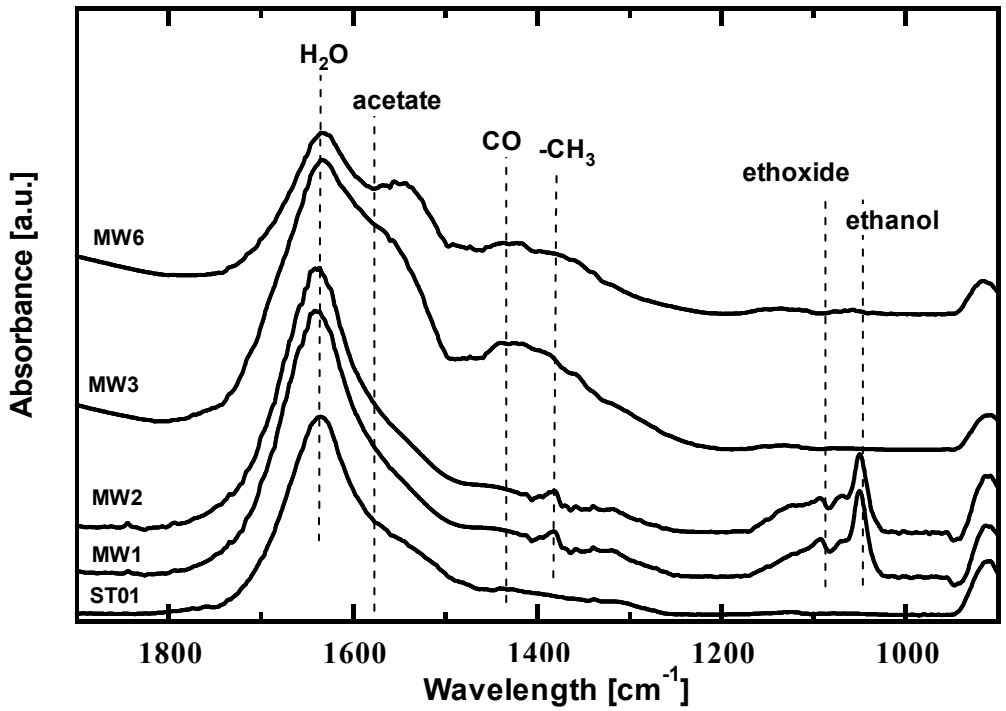

Fig. 2. ATR-FTIR spectra of untreated TiO_2 (ST01), and microwave treated TiO_2 for 1 (MW1), 2 (MW2), 3 (MW3), and 6 min (MW6)

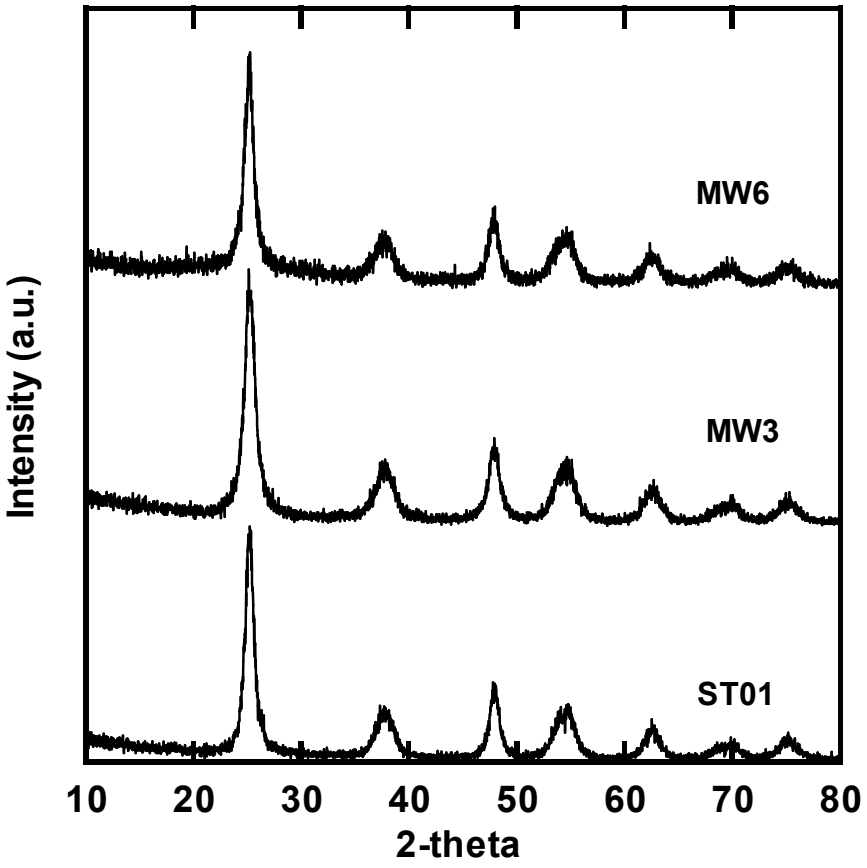

Fig. 3. XRD patterns of untreated TiO_2 (ST01), and microwave treated TiO_2 for 3 (MW3) and 6 (MW6) min.

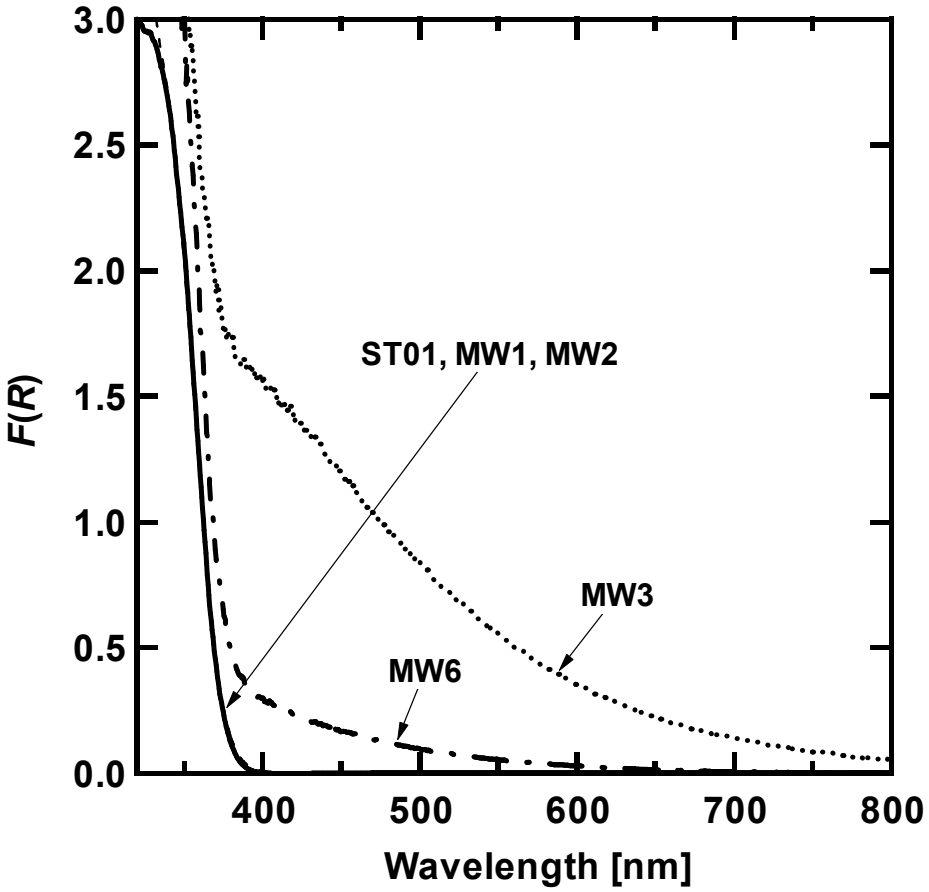

Fig. 4. UV-Vis absorption coefficients obtained from diffuse reflectance spectra with Kubelka-Munk relation for untreated TiO_2 (ST01), and microwave treated TiO_2 for 1 (MW1), 2 (MW2), 3 (MW3), and 6 (MW6) min.

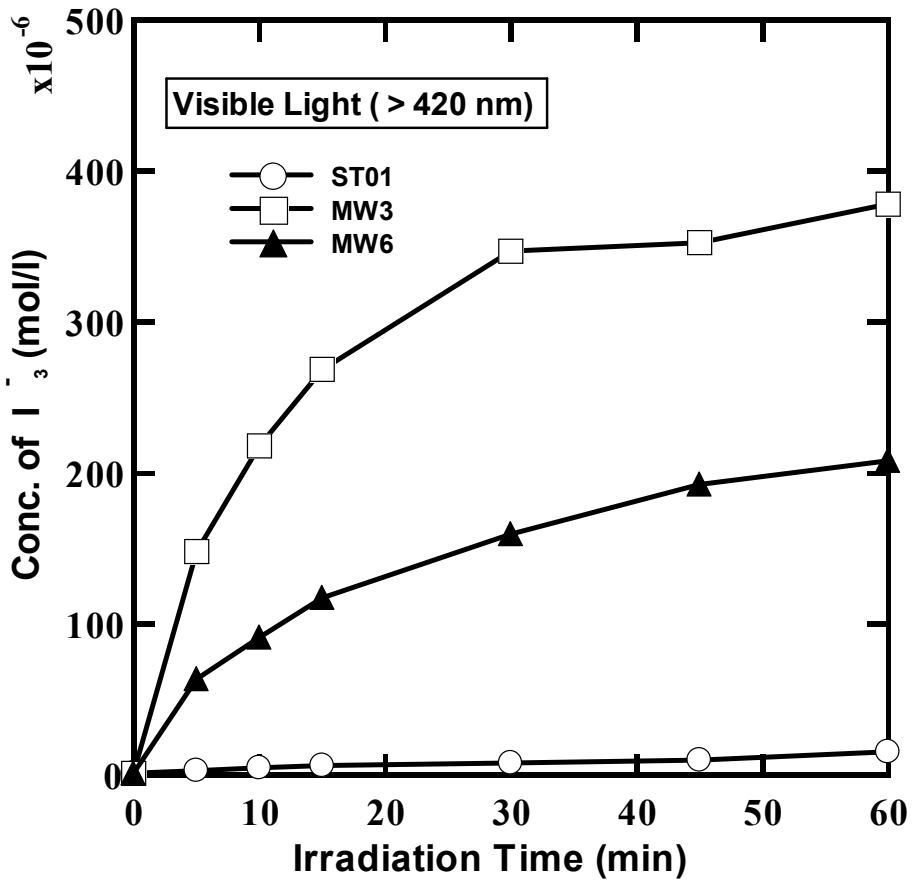

Fig. 5. Formation profiles of I_3^- as a function of visible light ($\lambda > 420$nm) irradiation time in the suspension of untreated TiO_2 (ST01), and microwave treated TiO_2 for 3 (MW3) and 6 (MW6) min.

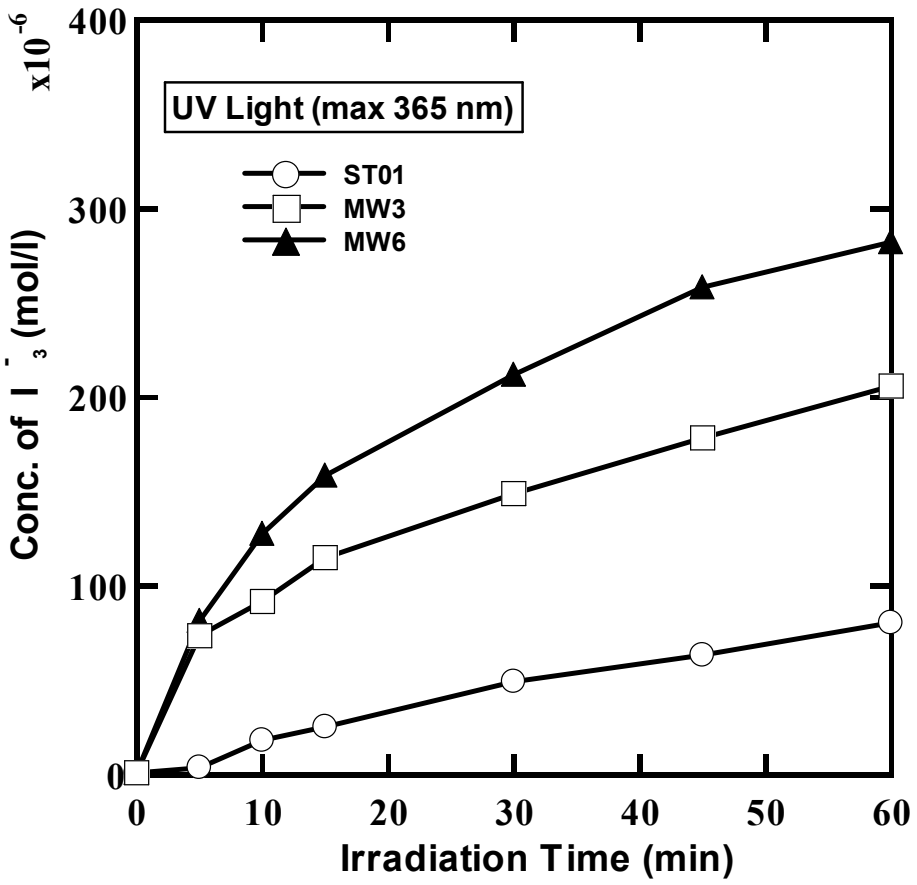

Fig. 6. Formation profiles of I_3^- as a function of UV irradiation time in the suspension of untreated TiO_2 (ST01), and microwave treated TiO_2 for 3 (MW3) and 6 (MW6) min.

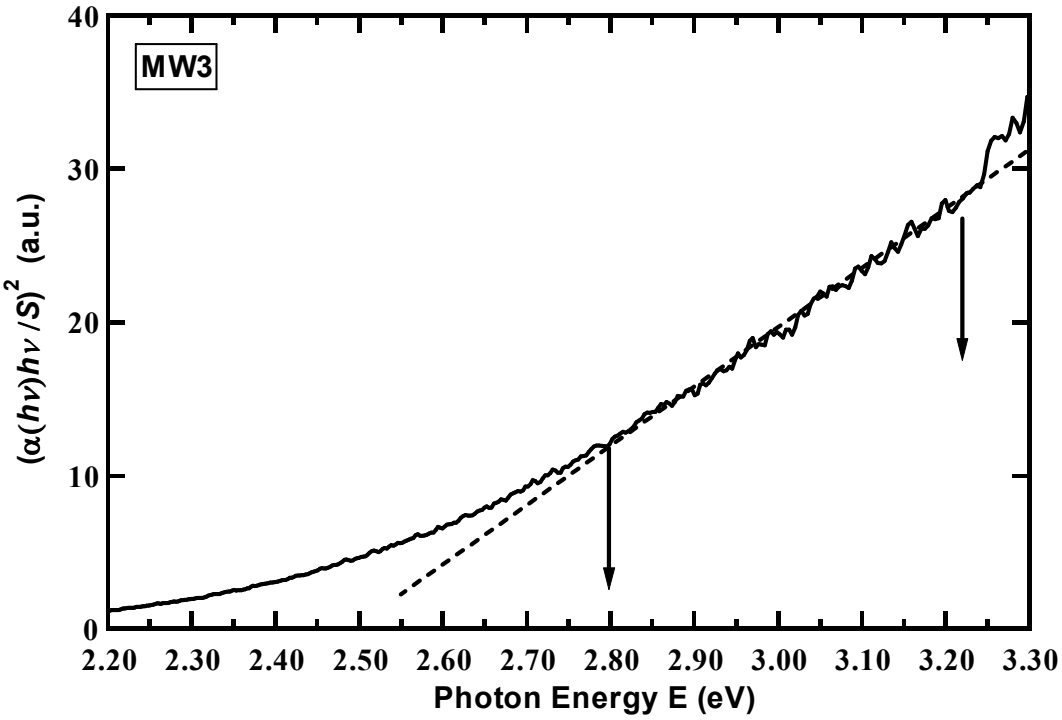

Fig. 7. The plot of $(\alpha h\nu/S)^2$ vs photon energy for the absorption edge of MW3 denoted by the solid curve. The dotted line is visual guides for $\alpha h\nu \propto (h\nu\text{-}E')^{1/2}$ and to evaluate the absorption threshold ($E' = E_g$ for bandgap absorption).

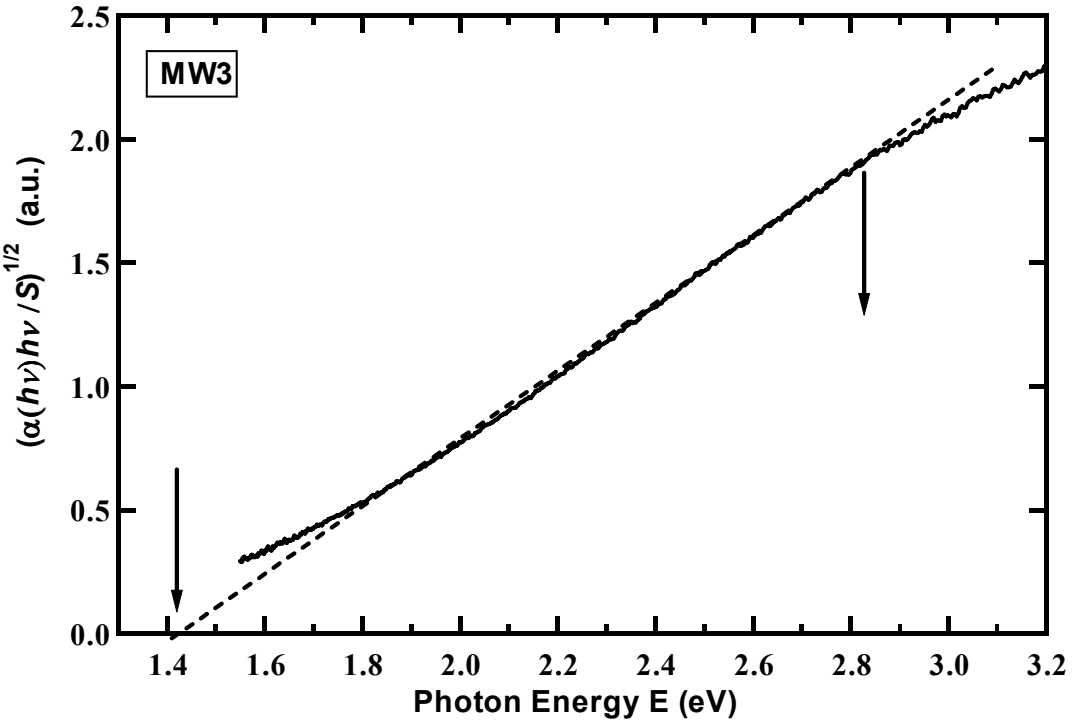

Fig. 8. The plot of $(\alpha h\nu/S)^{1/2}$ vs photon energy for the absorption edge of MW3 denoted by the solid curve. The dotted line is visual guides for $\alpha h\nu \propto (h\nu\text{-}E')^2$ and to evaluate the absorption threshold ($E' = E_g$ for bandgap absorption).

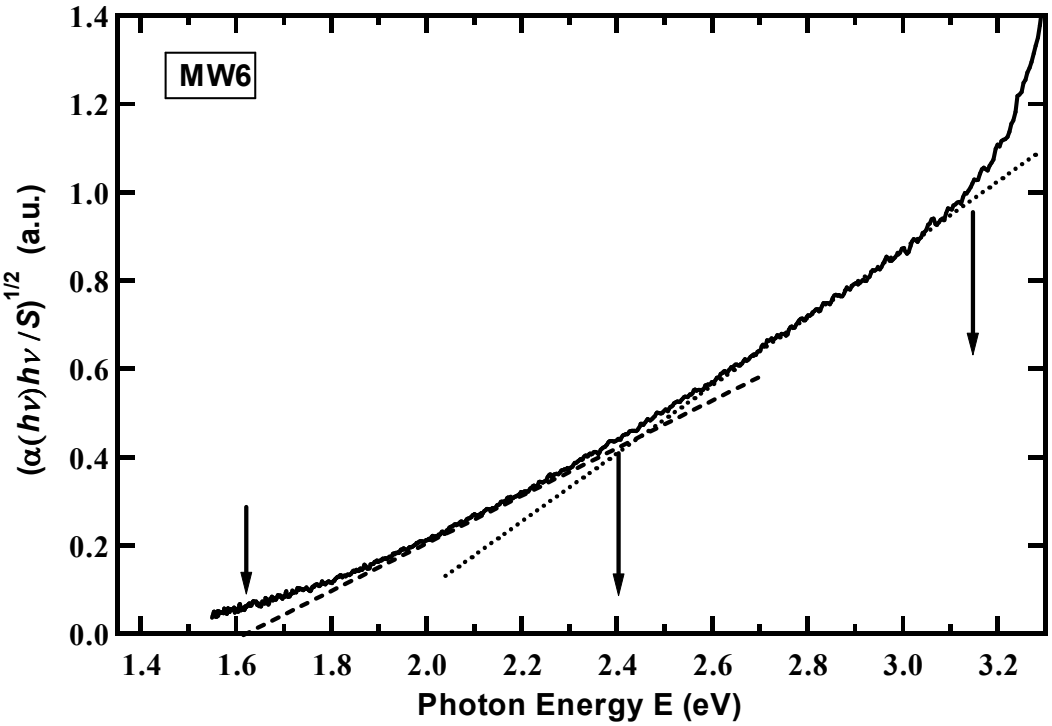

Fig. 9. The plot of $(\alpha h\nu/S)^{1/2}$ vs photon energy for the absorption edge of MW6 denoted by the solid curve. The dotted line is visual guides for $\alpha h\nu \propto (h\nu\text{-}E')^2$ and to evaluate the absorption threshold ($E' = E_g$ for bandgap absorption).